International Biodeterioration & Biodegradation 87 (2014) 87–98

Contents lists available at ScienceDirect

International Biodeterioration & Biodegradation

journal homepage: www.elsevier.com/locate/ibiod

Effects of biodegradation by brown-rot decay on selected wood properties in eastern white cedar (*Thuja occidentalis* L.)

Besma Bouslimi, Ahmed Koubaa*, Yves Bergeron

Forest Research Institute, Université du Québec in Abitibi-Téminscamingue, 445 boul. de l'Université, Rouyn-Noranda J9X 5E4, Québec, Canada

ARTICLE INFO

Article history:
Received 25 August 2013
Received in revised form
8 November 2013
Accepted 11 November 2013
Available online

Keywords:
Brown rot decay
X-ray densitometer
Scanning electron microscopy
Chemical properties
Mechanical properties

ABSTRACT

The effects of decay on wood density, wood structure, chemical composition, and mechanical properties in eastern white cedar (*Thuja occidentalis* L.) were investigated. Decay stage was determined by X-ray densitometry and scanning electron microscopy (SEM). Chemical and mechanical properties of decayed and sound wood samples were also determined. SEM results showed that decay colonization varied among wood cell types and within individual cell wall layers. Growth of fungi causing brown rot decay was limited and slower in latewood than in earlywood due to the narrow cell lumen, thicker wall, and higher density of latewood. Decay-related changes in wood density were more prominent in earlywood than latewood tracheids. Brown-rot decay selectively removes structural carbohydrate components, increasing the higher lignin/carbohydrate ratio as decay progresses. The relationships between chemical composition, mechanical properties, and weight loss were highly significant, with 15% weight loss leading to 40% loss in modulus of rupture (MOR) and 30% loss in bending modulus of elasticity (MOE). The strength loss (MOR) was attributable to arabinan and galactan loss. The loss in wood stiffness was associated with cellulose (glucan) loss, and weight loss was associated with mannan and xylans losses.
© 2013 Elsevier Ltd. All rights reserved.

1. Introduction and background

Natural durability or decay resistance is the ability of wood to withstand biological degradation (Schultz and Nicholas, 2000). Eastern white cedar (EWC) (*Thuja occidentalis* L.), one of only two arborvitae species native to North America, is considered one of the most durable woods in Canada (Taylor et al., 2002). Its timber, especially the heartwood components, has a natural durability that enhances its utility in wooden structures exposed to constant moisture (Taylor et al., 2002). For example, the average service life of an untreated EWC post is 27 years, compared to just five years for a black spruce (*Picea mariana* (Mill.) B.S.P.) post (Koubaa and Zhang, 2008). Hence, products such as shakes, shingles, fence posts, and mulch made with EWC have considerable potential market value (Behr, 1976; Haataja and Laks, 1995). EWC timber has been used to improve the ability of medium-density fiberboard (MDF) (Behr, 1976), oriented strand board (OSB) (Wan et al., 2007), and flakeboard to withstand decay and termites (Haataja and Laks, 1995). The resistance of EWC to microbial attack and decay is due to the presence of toxic extractives in the heartwood (Taylor et al., 2002). However, even the most decay-resistant woods are susceptible to rot under certain combined moisture and temperature conditions. However, butt and root rots do attack EWC, and among them are a white, stringy butt rot, *Poria subacida*, and brown cubical rots, *Polyporus balsameus* and *Phaeolus scheweinnitzii* (Fowells, 1965; Johnston and Booker, 1983; Koubaa and Zhang, 2008).

The capacity of rot fungi to degrade wood varies among fungal species and depends on the structure and chemical properties of the wood components. The EWC wood contains about 30–32% of lignin, 72% of holocellulose and 43–48% of cellulose (Timell, 1957). The total cellulose was the predominant polysaccharide type in EWC and was in the same level in heartwood and sapwood. The carbohydrate composition suggested that the main non-cellulose polysaccharides were galacto-glucomannan (Rowell et al., 2005). The content of xylans was in the same range as the mannans in EWC heartwood and sapwood (Willför et al., 2005). This species wood contained 7.2% mannose, 1.7% arabinogalactans and 1.8% pectins (Willför et al., 2005).

A natural resistance to decay is one of the most attractive properties of wood, and is mainly attributable to its lignin and extractives contents (Oliveira et al., 2010). After cellulose, lignin is the second most abundant type of biopolymers on the earth and provides plant resistance to microbial degradation, markedly influencing the natural durability of wood (Syafii and Yoshimoto, 1991; Gierlinger et al., 2004). Although extractives make up only

* Corresponding author. Tel.: +1 819 762 0971x2579; fax: +1 819 797 4727.
E-mail addresses: besma.bouslimi@uqat.ca (B. Bouslimi), ahmed.koubaa@uqat.ca (A. Koubaa), yves.bergeron@uqat.ca (Y. Bergeron).

0964-8305/$ – see front matter © 2013 Elsevier Ltd. All rights reserved.
http://dx.doi.org/10.1016/j.ibiod.2013.11.006

a small percent of the total wood composition, they provide trees with invaluable defense mechanisms against microbial attack, thanks to their fungicidal and antioxidant properties (Silva et al., 2007; Curnel et al., 2008). Extractives performance as antioxidants is due to the presence of aromatic hydroxyl groups, which enable them to scavenge free radicals (Amusant et al., 2007; Oliveira et al., 2010).

The EWC heartwood is valued for the natural durability conferred by fungicidal agents in its extractives in particular, by a group of tropolone compounds known as thujaplicins (Taylor et al., 2002, 2006; Willför et al., 2003). According to Willför et al. (2003), thujalignans were the main compounds in EWC *and responsible for* the antioxidant potency.

In living trees, wood decay is initiated by hyphal penetration of cell walls (Kleist and Seehann, 1997; Kleist and Schmitt, 2001; Silva Pereira et al., 2006). The fungi then secrete enzymes that facilitate wood decay by oxidizing side chains of aromatic wood compounds, rendering them less toxic to fungi. The contamination of heartwood therefore advances from the centre outward (Amusant et al., 2004). Although the decay process varies with the species, it generally progresses sequentially as incipient, intermediate, and advanced decay. According to different physical, chemical, and morphological changes in the wood, the decay may be accompanied by substantial decreases in mechanical properties resulting from only modest losses in wood components (Smith and Graham, 1983; Green III and Highley, 1997; Curling et al., 2002; Clausen and Kartal, 2003; Yang et al., 2010). This alteration directly impacts structural uses of the wood due to the risks of sudden failure of sound material (Winandy and Morrell, 1993). Although considerable efforts have been made in the last two decades to understand the nature of these dramatic changes in wood properties, the extent and the precise mechanisms of the effects on structural strength remain unknown.

According to macroscopic differences, rotted wood is classified into three decay groups: white rot, brown rot, and soft rot fungi (Martínez et al., 2005). In general, any decay that becomes progressive in the central dead wood of a living tree is called heart rot. EWC is highly susceptible to heart rot, which can cause significant losses in structural integrity and predisposes infected trees to windthrow (Hofmeyer et al., 2009). Brown-rot decay is the most common decay type in EWC (Koubaa and Zhang, 2008).

Several studies have examined the effects of brown-rot decay on wood mechanical and chemical properties under laboratory conditions (Winandy and Morrell, 1993; Curling et al., 2002; Clausen and Kartal, 2003; Silva Pereira et al., 2006; Silva et al., 2007). Brown-rot decay appears to metabolize lignocellulose carbohydrates without removing lignin, leading to a rapid decrease in the degree of polymerization at low weight loss (Green III and Highley, 1997; Schilling et al., 2009; Howell et al., 2011; Hastrup et al., 2012).

A few studies have investigated the macroscopic and microscopic structure of sound and brown-rot decayed wood in EWC (Bouslimi et al., 2013), but no study to date has investigated changes in physical, chemical, and mechanical properties due to decay in EWC wood. Although few studies linked the mechanical properties changes to the variation of chemical composition in few wood species, there are no studies that examined the relationship between the decay-related changes in the mechanical properties and the different wood polymers. Thus, the main objective of this study was therefore to analyze the effects of brown-rot decay on EWC wood properties. The specific objectives were 1) to determine the effect of decay on wood physical, morphological, chemical, and mechanical properties; and 2) to investigate the impact of decay-related chemical changes on wood mechanical properties.

2. Material and methods

2.1. Study material

Samples were obtained from 45 trees randomly selected from three mature EWC stands in the Abitibi-Témiscamingue region in the province of Quebec, Canada: [Abitibi (48°.28′N, 79°.27′W); Lac Duparquet (48°.25′N,79°.24′W) and Témiscamingue (47°.25′N, 78°.40′W)]. Site location and tree characteristics were described in Bouslimi et al. (2013). The age of sampled trees ranged from 60 to 198 years, with an average age of 93, 121 and 93 years for Abitibi, Lac Duparquet and Témiscamingue sites, respectively. The ring width of sampled trees ranged from 0.12 to 4.6 mm, with an average ring width of 1.21, 0.93 and 0.95 mm for Abitibi, Lac Duparquet and Témiscamingue sites, respectively. The decay in sampled trees is limited to the heartwood, and characterized by brown discoloration and a friable, cubically cracked texture when dry (Bouslimi et al., 2013). In very advanced decay, cracks appeared in the decayed wood and the wood is completely degraded.

The sampled trees (15 trees per site) were felled and the log between 1.4-m and 3-m stem height was sawed into planks 1¼ inch thick. Samples were extracted from the planks for mechanical testing. A 10-cm-thick disk was sampled from each tree at breast height (1.3 m) and air-dried for several months until sample preparation and analysis. Samples were extracted from these disks for chemical testing. From the sampled disk, 1 cm width and 5 cm depth pith-to-bark planks were sawn to extract test samples for physical, anatomical and chemical properties measurement. The decay class of each sample was determined by from X-ray density according to the procedure described in Section 2.3.

2.2. Wood density measurement

To determine wood density, thin strips 20 mm wide and 1.57 mm thick were sawn from each breast-height plank (bark to bark passing through the pith). The strips were then extracted with cyclohexane/ethanol solution 2:1 (v/v) for 24 h and with distilled water for another 24 h to remove resinous substances and water-soluble carbohydrates (Grabner et al., 2005). The extractives were removed to control for their effect on wood density in order to more accurately compare changes in wood density with decay incidence.

Wood density characteristics were determined using a QTRS-01X Tree-Ring X-Ray Scanner (QMC, Knoxville, Tennessee). A linear resolution step size of 20 μm was used for X-ray densitometry. The mass attenuation coefficient (cm^2/g) required to calculate the density was determined on a set of 20 radial strips from cores with previously determined densities using the maximum moisture content method (Guller et al., 2012). After conditioning, rings from the pith to the bark were scanned in air-dry condition. From the wood density profiles, average density (RD), earlywood density (EWD), and latewood density (LWD) were calculated for each annual ring. Demarcation between earlywood and latewood was determined for each annual ring by the maximum derivative method using a six-degree polynomial (Koubaa et al., 2002). During scanning, precautions were taken to eliminate incomplete or false rings and rings with compression wood or branch tracers.

2.3. Decay classification

X-ray densitometry profiling was used for decay stages determination of each plank. The classification is based on visual examination of the profile and density reduction compared to density average of the sound samples. Decay samples clearly indicated a lower density profiles compared to sound samples (see Section 3.2). Depending on the amplitude of reduction samples were divided

into three groups: sound or undecayed (C0); early stage decay (C1); and advanced stage decay (C2). Sound samples are those that do not show any visible profile change and present marginal density change (less than 2%). The early stage refers to the incipient stage of wood colonization (or initial decay), which was estimated at 2–15% wood density loss. In the studied C1 samples, the density reduction ranged from 2% to 8%. The second stage (advanced decay) was estimated at density reduction higher than 15%. In the studied C2 samples, the density reduction ranged from 30 to 50%. Considering, the large differences in density change among the three classes, the distinction between these classes is clear.

2.4. Scanning electron microscopy (SEM) analysis

For each decay stage, two small heartwood specimens (2.5 by 2.5 by 1 cm) were cut from sampled planks and prepared for SEM testing. Specimens were first softened by overnight soaking in water and then oven-dried for 2 h at 100 °C. The area of interest was cut out with a razor and platinum deposits followed by carbon deposits were applied to the surface. The surfaces were then observed using a scanning electron microscope (JSM-840A, SRNEML, Oklahoma, USA).

2.5. Chemical analysis

From the sampled planks, wood blocks (2.5 by 2.5 by 1 cm) from the three groups of heartwood (sound, initial decay, and advanced decay) and from the sapwood were cross-cut from breast-height disks, dried at 50 °C for 72 h, and weighed. The samples were then ground to pass through a 40-mesh screen (according to TAPPI T264 om-88 (1989)) and the powder was stored over a desiccant. The obtained powder was used to determine extractive, lignin, cellulose, hemicellulose, and carbohydrate (arabinan, galactan, mannan, xylans, and glucan) fractions (% oven-dry weight) for each group. In all, 30 samples were analyzed (12 sound heartwood and 12 sapwood, 3 initial decay and 3 advanced decay).

Chemical analyses were conducted in 2 replicates according to TAPPI test methods. Lignin content was determined as the summation of acid-insoluble lignin (or klason lignin according to TAPPI T 222 om-88 (1989), and acid-soluble lignin according to TAPPI useful method UM 250). Cellulose content was determined according to the Kurschner–Hoffner method (Browning, 1967). Carbohydrate content was determined according to Tappi standard method T249 cm-85 (1989) using high-performance liquid chromatography (Schilling et al., 2009). Glucose, xylose, galactose, arabinose, and mannose were quantified according to previously described procedures (Kartal et al., 2008; Schilling et al., 2009). The percent glucose content in the hemicelluloses was estimated based on a 2:1 ratio for mannose/glucose and 10:1 for xylose/glucose. The cellulose fraction was then calculated as the difference between total glucose content and glucose associated with hemicelluloses.

Water solubility was determined according to TAPPI T 207 om-88 (1989). To determine cold water solubility, 10 g of wood powder was extracted with 300 ml distilled cold-water at 23 °C with stirring for 48 h. To determine hot water solubility, wood was extracted with 100 ml water under reflux in a boiling water bath for 3 h. Extracts were dried to a constant weight and the oven-dry weight of extracts was determined.

For all analyses, the composition (extractive, lignin, cellulose, hemicellulose, and carbohydrate contents) is expressed based on the biomass dry weight, which was determined by drying the biomass (extracts) to a constant weight at 103 °C. Results were reported as the percentage of the original sample mass. Extractive, lignin, cellulose, hemicellulose, and carbohydrate fractions (in %) of decayed samples (C1 and C2) were compared with undecayed samples (C0) to determine the loss rate of these properties.

2.6. Wood mechanical properties measurement

Planks obtained from the log extracted between 1.4 m and 3 m height were processed to obtain clear wood samples for parallel and perpendicular-to-grain compression tests, three bending tests, and hardness tests. For each test, two to five replicates were used, depending on plank quality and tree diameter. Test samples dimensions were according to ASTM Standard D143. Air-dried decayed and undecayed clear wood samples were conditioned at 20 ± 3 °C and 65 ± 3% relative humidity for 3 months to reach an equilibrium moisture content of 7%. The tested mechanical properties included the modulus of elasticity (MOE) and the bending modulus of rupture (MOR), the maximum compressive strength parallel to grain compression (MS), the stress at the limit of elasticity in perpendicular compression (LS), and hardness. A universal testing machine (ZWICK, Germany) with 100 kN capacity was used for perpendicular and parallel compression testing. Another universal testing machine with 20 kN capacity (ZWICK, Germany) was used for the hardness and the three bending tests. Test sample dimensions were measured to the nearest 0.01 mm and weighed to the nearest 0.01 g for apparent density determination. After testing, all samples were oven-dried for 24 h at 103 °C to a constant weight and weighed to determine moisture content. For each decay class, averages of all mechanical properties were determined. The relative ratio of the loss in mechanical properties to weight loss (i.e., strength/weight loss) was calculated. Strength loss is reported as the difference in average strength properties between each decayed sample and the undecayed samples.

2.7. Statistical analysis

Wood density components (RD, EWD, and LWD) were subjected to variance analyses (ANOVA) using a mixed-model approach, with cambial age as the repeated measure (Littell et al., 2006). All trees had at least 58 annual rings. However, data beyond the 25th annual ring were not considered in the analysis. Because the first annual ring was not included in the analysis, data included 19 repeated measures (from ring 2 to 20). All factors were considered fixed effects (decay class, site, cambial age, and tree). Only significant interactions were retained in the model. The hierarchical effects of individual tree and site were accounted for using two nested levels, with the tree effect nested within the site effect, as follows (Eq. (1)):

$$Y_{ijkl} = \mu + \alpha_i + \beta_j + \gamma_k + \delta_l + (\alpha\beta)_{ij} + (\alpha\delta)_{il} + \varepsilon \quad (1)$$

where Y is the dependent variable, μ the grand mean, α_i the fixed effect of decay class, β_j the fixed effect of cambial age, $(\alpha\beta)_{ij}$ the interaction between decay class and cambial age, γ_k the fixed site effect, δ_l the fixed tree effect, $(\alpha\delta)_{il}$ the interaction between decay class and tree, and ε the residual error. Data were analyzed using SAS (SAS, 2008). The mixed-model procedure (PROC MIXED) was used to fit models using restricted maximum likelihood (REML). Degrees of freedom were determined using the Kenward–Roger method (Littell et al., 2006). The statistical significance of fixed effects was determined using F-tests at $p \leq 0.05$. Variance components were estimated as a percentage of total variation (VAR) of all effects, using the VAR COMP procedure. In all, 45 samples were analyzed (13 sound wood, 16 initial decay, and 16 advanced decay).

The mean and the standard deviation for each wood property (physical, chemical, and mechanical) were calculated for each decay class. Tukey's multiple range method was used to test significant statistical differences in physical, mechanical, and chemical properties between decay classes. Values were considered statistically significant at $p \leq 0.05$. Correlation analyses were also conducted using the CORR procedure to determine relationships between chemical composition, mechanical properties, and weight loss.

3. Results

3.1. Microscopic structure of sound and decayed heartwood

Sound heartwood in *T. occidentalis* L. is relatively homogeneous and simple in structure, consisting primarily of overlapping tracheids connected by bordered pits and parenchyma cells (Fig. 1A and B). The tracheid cell walls are organized in layers of different thickness: thick latewood cell walls and thin earlywood

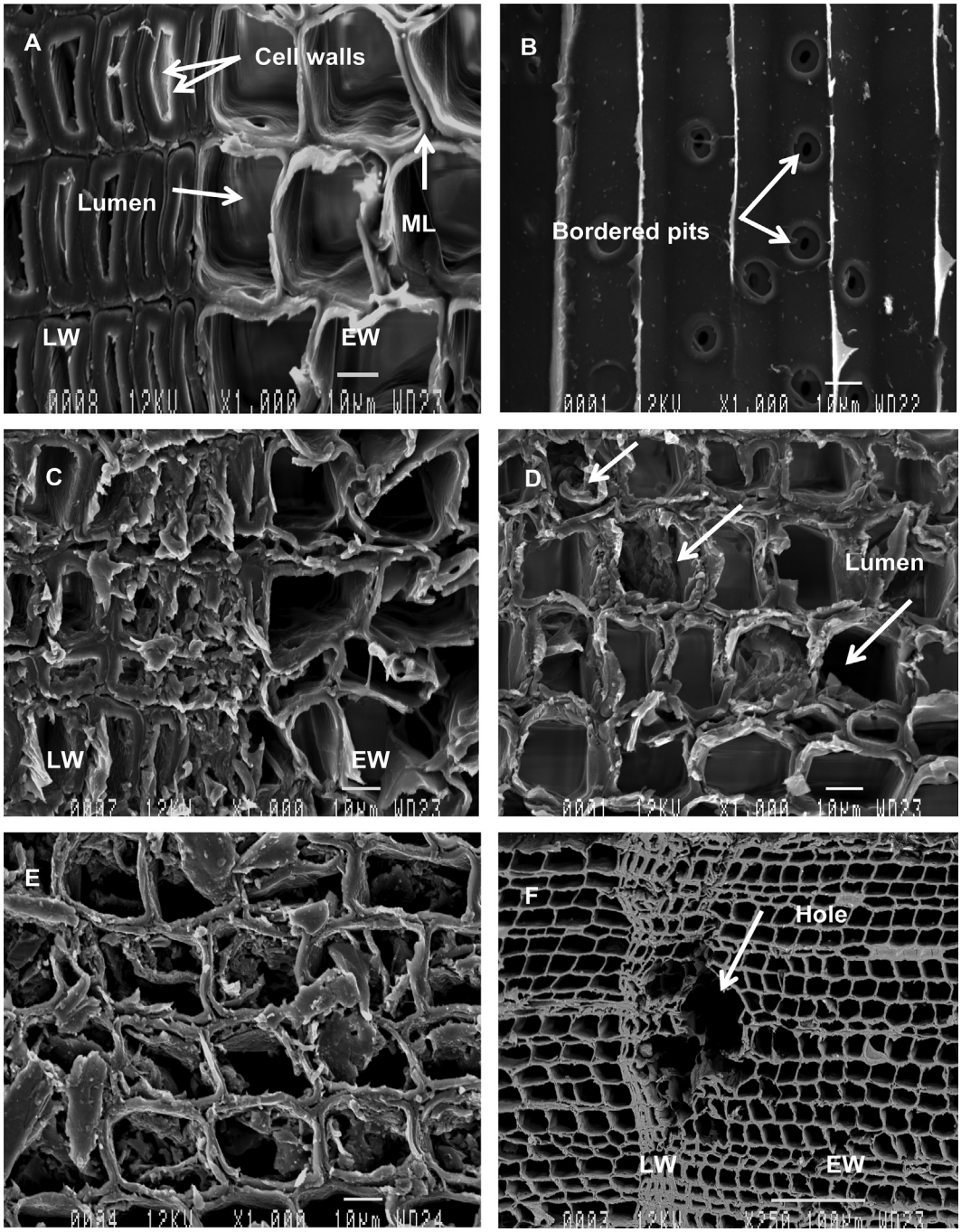

Fig. 1. Cell structure of sound (A and B) and decayed (C, D, E and F) heartwood in *Thuja occidentalis* L.: A. Transverse section showing cell walls, middle lamella (ML), and lumen in earlywood (EW) and latewood (LW) tracheids. B. Radial section showing bordered pits in earlywood tracheids. C. Transverse section showing rapid decay growth in the cell lumina of earlywood tracheids (EW) compared to latewood tracheids (LW). D. Transverse section showing the progressive degradation of cell lumina in earlywood tracheids. E. Transverse section showing substantial degradation of lumen, cell walls, and middle lamella in earlywood tracheids. F. Transverse section showing porous areas in both earlywood and latewood tracheids in advanced decay.

cell walls (Fig. 1A). The cell walls surround the lumen, and the walls of adjacent cells are bonded together by the middle lamella (Fig. 1A). Latewood tracheids are characterized by narrow cell lumina and thick cell walls (Fig. 1A).

The structure of decayed heartwood shows that the fungal growth occurred rapidly within the broad cell lumina of the earlywood tracheids (Fig. 1C and D), causing a progressive degradation of lumen (Fig. 1D). The initial decay is more extensive in earlywood than in latewood (Fig. 1C). In advanced decay, earlywood cells show substantial degradation (Fig. 1E), which has extended to latewood cells (Fig. 1F). This degradation has produced porous zones in the earlywood and latewood tissues in the advanced stage of decay, which typically leads to the development of holes and cracks (Fig. 1F).

In initial decay, the degradation occurred within the broad cell lumina of the earlywood tracheids, but degradation has not extended to the middle lamella and cell walls (Fig. 1D). As the decay progresses, the secondary wall degrades progressively from cell lumina toward the middle lamellae (Fig. 1D and E) in both earlywood and latewood tracheids.

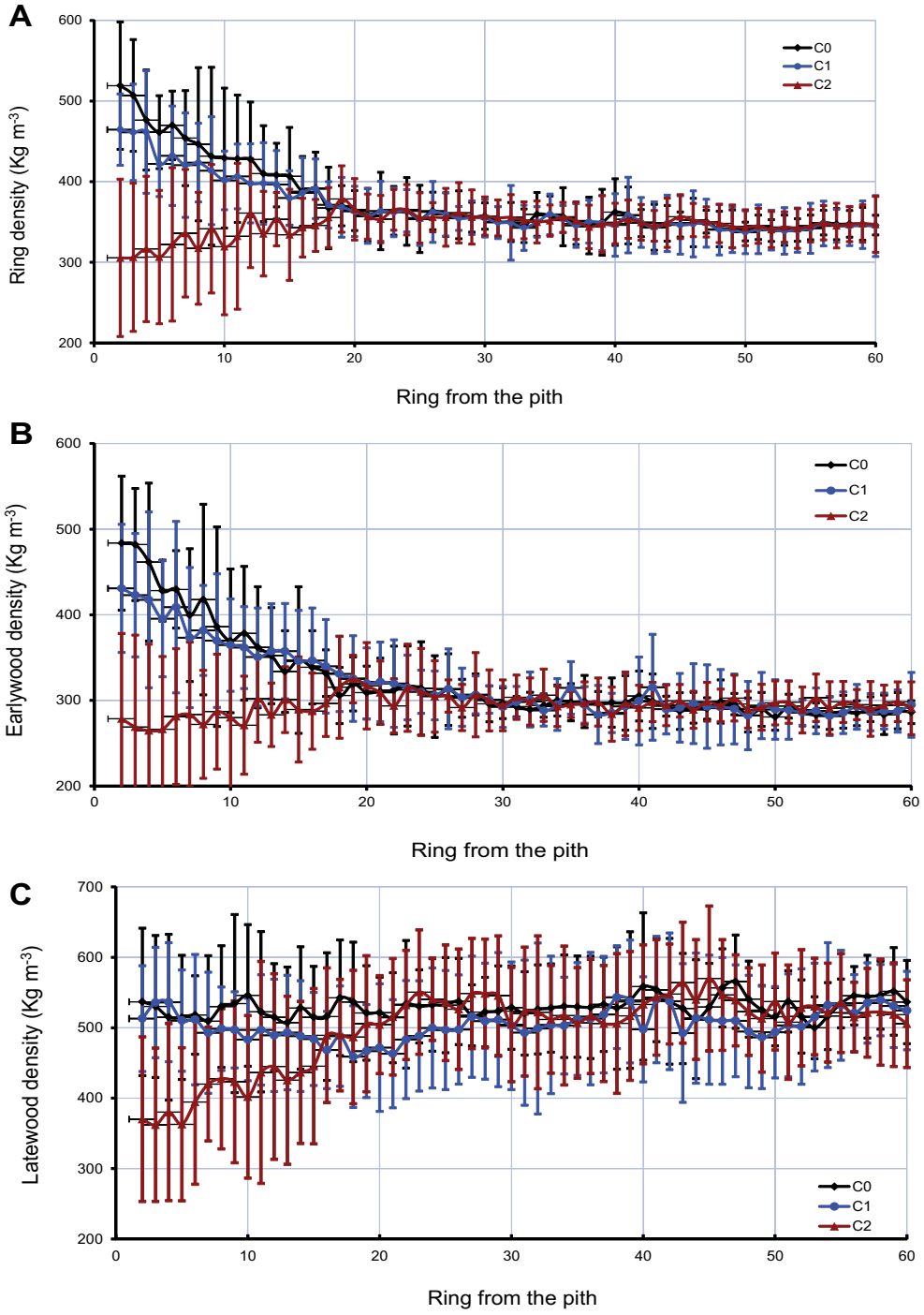

Fig. 2. Variation of average ring density (A), earlywood density (B) and latewood density (C) as related to decay class[a] (C0, C1 and C2) and ring from the pith in *Thuja occidentalis* L.
[a]Decay class: C0 = sound wood; C1 = initial stage of decay and C2 = advanced stage of decay.

At advanced decay stages, the wood cell integrity is compromised, indicating the physical weakness of the compounds in the middle lamella (Fig. 1E). The cellulose and hemicelluloses in the wood fibers have largely decomposed, leaving a fragile framework of lignin (Fig. 1E). Without cellulose, wood fibers lack integrity, such that at more advanced stages of decay, the degraded wood area grows larger and holes are formed (Fig. 1F). Cracks often develop between adjacent holes in the radial cell walls, and the holes eventually coalesce into a single large hole (Fig. 1F).

3.2. Effect of brown-rot decay on ring density

The patterns of radial variation in ring density (RD), earlywood density (EWD), and latewood (LWD) density of sound and decayed wood of *T. occidentalis* L. are presented in Fig. 2. RD profiles vary substantially between sound wood (C0), early decay (C1), and advanced decay (C2) samples (Fig. 2A). For sound wood, RD is high near the pith and decreases slowly thereafter to reach a minimum in the juvenile–mature wood transition zone. In the mature wood zone, RD remains constant or decreases slightly. The RD pattern for early decayed wood is similar to that for sound wood, with a slight decrease in density in the first 20 rings. For advanced decay samples, RD is considerably lower in the first 20 rings. Beyond the 20th ring, the density of both initial and advanced areas of decay is similar to that of sound wood (Fig. 2A).

The patterns of EWD variation in the three decay classes are similar to the RD patterns (Fig. 2B). The LWD patterns for sound wood and the initial decay class are typical of that for LWD radial variation, which is characterized by constancy over the tree age (Koubaa and Zhang, 2008). However, for the advanced decay class, the LWD is low near the pith, increasing thereafter to reach a maximum around the 20th ring from pith, and remaining constant outward (Fig. 2C).

The analysis of variance (Table 1) in the RD of the first 20 rings revealed a significant difference ($p \leq 0.001$) across the three decay classes (C0, C1, and C2). The interaction between decay class and cambial age was the main source of variation, accounting for 28% of the total variation (Table 1). The site effect was not statically significant, and could be masked by within-tree variation, mainly the variation between juvenile and mature wood and the presence of compression wood (Koubaa et al., 2000). The significant tree effect could also partially explain this result (Table 1). Despite the variation in site properties (Bouslimi et al., 2013), the site effect could be masked by tree-to-tree variation. The tree effect on RD was highly significant ($p < 0.001$) (Table 1). The greater tree variation in RD was associated with a large standard deviation (Table 1 and Fig. 2A). The cambial age effect was also highly significant, explaining 8% of the total variation. This effect was associated with RD variation between juvenile and mature wood (Fig. 2A). Similar results were obtained for EWD and LWD (Table 1).

The interaction between decay class and cambial age was highly significant (Table 1) for RD. This could be explained by the radial variation patterns of RD, which differed across the three decay classes (Fig. 2A). The sound and early decay samples showed similar trends, with decreasing RD from the pith outward. The early decay curve is slightly lower than the sound wood curve. However, the advanced decay curve shows a completely different trend (Fig. 2A), increasing slightly from the pith to about the 20th ring and tending to remain constant outward thereafter. Similar results to RD were found for EWD and LWD (Fig. 2B and C).

The tree effect on RD, EWD, and LWD was highly significant, although it accounted for only a small proportion of the total

Table 2
Means, standard deviation (SD) and reduction (in percent) of average ring density (RD), earlywood density (EWD) and latewood density (LWD) as related to decay class (C0, C1 and C2) and ring from the pith, in *Thuja occidentalis* L.

Decay class[b]	Ring from pith					All rings	
	2–5	5–10	10–15	15–20	20–25	2–20	
	Reduction[a]					Means	SD
Average ring density							
C0	0^{A}	0^{A}	0^{A}	0^{A}	0^{A}	427.8	75.4
C1	8.8^{A}	6.6^{A}	5.4^{A}	1.5^{A}	0.2^{A}	403.8	53.4
C2	37.3^{B}	27.8^{B}	19.2^{B}	7.4^{B}	0.3^{A}	337.0	68.9
Earlywood density							
C0	0^{A}	0^{A}	0^{A}	0^{A}	0^{A}	379.2	84.7
C1	10.3^{A}	5.8^{A}	0.2^{A}	2.9^{A}	1.3^{A}	363.6	68.5
C2	41.8^{B}	31.2^{B}	24.5^{B}	8.8^{B}	2.2^{A}	289.1	67.4
Latewood density							
C0	0^{A}	0^{A}	0^{A}	0^{A}	0^{A}	521.9	88.2
C1	0.12^{A}	3.7^{A}	6.3^{A}	7.4^{A}	8.2^{B}	491	75.5
C2	29.6^{B}	21.6^{B}	17.2^{B}	10.0^{B}	0.5^{A}	435.5	114.1

Values with different letters are significantly different at $p < 0.05$.
[a] The reduction of RD, EWD and EWD of decayed woods (C1 and C2) was calculated compared to mean RD, EWD and LWD of sound sample (C0) as related to ring from the pith.
[b] Decay class: C0 = Control or sound wood; C1 = Initial stage of decay and C2 = Advanced stage of decay.

Table 1
Linear mixed model analysis of variance; showing *F* values for fixed effects, *Z* values for random effects, their significance, and the variance component (VAR COMP) of each source of variation for wood density (RD), earlywood density (EWD) and latewood density (LWD) of the twenty initial rings (from the pith) for *Thuja occidentalis* L.

	df[a]	Ring density			Earlywood density			Latewood density		
		F value	*p* Value	VAR COMP (%)	*F* value	*p* Value	VAR COMP (%)	*F* value	*p* Value	VAR COMP (%)
Fixed effects										
Decay class (DC)	2	38.22	<0.0001	6.4	28.86	<0.0001	5.1	5.25	0.0085	0
Cambial age (CA)	18	2.93	<0.0001	7.8	3.07	<0.0001	12.8	0.57	0.91	1.4
Site	2	0.84	0.43	0	0.26	0.77	0.3	1.25	0.29	2.8
Tree	14	5.06	<0.0001	0.17	2.99	0.0012	0.0	3.32	0.0008	7
DC × CA[b]	36	2.81	<0.0001	27.7	2.14	0.0002	24.6	1.52	0.029	8.9
DC × Tree[c]	28	2.31	0.0106	5.7	1.93	0.0363	5.1	3.84	0.0002	15.9
		Z value	*p* Value	VAR COMP (%)	*Z* value	*p* Value	VAR COMP (%)	*Z* value	*p* Value	VAR COMP (%)
Random effects										
Residual	597	11.93	<0.0001	51.9	11.61	<0.0001	52	9.44	<0.0001	63.8

[a] Degree of freedom.
[b] Interaction between decay class (DC) and cambial age (CA).
[c] Interaction between decay class (DC) and tree.

variation (Table 1). The between-tree variation, however, was greater in LWD than in EWD. It accounted for 7% and 0.03% of the LWD and EWD variation, respectively (Table 1). For EWD, the low tree variation could be explained by the greater EWD variation with cambial age (13% of the total variation). However, LWD is characterized by constancy over the cambial age, which helps explain the tree differences (Fig. 2C and Table 1). The interaction between decay class and tree was also highly significant, accounting for a large proportion of the total variation (5.8% for RD, 5.1% For EWD, and 15.9% for LWD).

Changes in density components related to decay class and ring number from the pith are presented in Table 2 . The reduction in EWD was more prominent than for LWD. Importantly, note that the reductions in wood components (RD, EWD, and LWD) were greater near the pith, decreasing thereafter with increasing ring number from the pith to ring 25 (Fig. 2 and Table 2), where the variations became non-significant (Fig. 2). The development of decay in the living wood began from the pith and decreased from inner to outer heartwood (Fig. 2). However, for all analyzed samples, decay did not occur in sapwood.

3.3. Effect of brown-rot decay on the chemical composition of heartwood

The chemical composition of sound and decayed heartwood and sapwood in EWC is presented in Table 3. For sound heartwood, the total extractive content was 14.1%, composed of 4.3% cold water soluble extractives (CWE) and 9.8% hot water soluble extractives (HWE). The lignin and cellulose content was 31.5% and 38.8%, respectively. The hemicellulose content was 15.5%. The total extractive content for sapwood (Table 3) was consistently lower (6.5%) than that for heartwood (14.1%). However, hemicellulose content was higher (19.2%) in sapwood than in heartwood (15.5%). The presence of brown-rot decay was associated with substantial changes in the chemical composition (Table 3): extractive content decreased slightly with decay class (from 14.1% in sound heartwood to 13.9% in decayed heartwood).

Results also revealed that cellulose and hemicellulose content decreased with decay class, whereas lignin content increased slightly (Table 3). At initial decay, hemicellulose content decreased by 16.4%, while cellulose content decreased by only 1.2% (Table 3), suggesting that during initial decay, hemicelluloses are degraded more rapidly than cellulose. In advanced decay, cellulose content showed a greater decrease (21.4%), suggesting a preferential degradation of cellulose by brown-rot decay. The lignin content increased during the decay process up to 33.3% (Table 3). The apparent increase in klason lignin is due in part to the ongoing removal of hemicelluloses as it degrades.

The presence of brown-rot decay was also associated with substantial changes in carbohydrate components (Table 3). However, there was variation in the relative extent of removal of these components (Table 3). The average loss varied between carbohydrate components, with arabinan and galactan showing the most degradation, followed by mannan and xylans. At early decay, approximately 31.1% of the arabinan and 27.9% of the galactan were degraded compared to 9.9% of the mannan and 7.5% of the xylans. It is also noteworthy that only 3.7% of the glucan, as a gross measure of cellulose, was degraded during incipient decay. Furthermore, mannan showed a greater decrease compared to xylans at initial decay, and this trend increased as decay progressed (Table 3): at advanced decay, approximately 16.7% of the mannan was degraded compared to 8.9% of the xylans.

3.4. Effect of brown-rot decay on wood mechanical properties

Decay caused a remarkable decrease in weight and mechanical properties (Table 4). At initial decay, MOR showed more rapid loss (21.5%) compared to MOE (17.4%). Results also revealed a significant negative impact of brown-rot decay on all tested mechanical properties (23.7% for LS, 19.9% for surface hardness, and 12.4% for MS). For all tested samples, weight loss was modest (6–10%) in incipient decay, suggesting that mechanical properties were lost at a faster rate than weight was lost (Table 4). The relative ratios of loss in mechanical properties to weight loss (i.e., strength/weight loss) are summarized in Table 5. At 6% weight loss, the strength/weight loss ratio was 3.4:1 for MOR and 2.8:1 for MOE. The relationships between weight and mechanical property losses were positively and strongly correlated ($p < 0.001$) (Table 5), with coefficients of correlation (r) of 0.71 for MOE, 0.54 for MOR, 0.71 for MS, 0.80 for LS, and 0.72 for end hardness.

Table 3
Chemical properties of sound and decayed heartwood and sapwood in *Thuja occidentalis* L.

Properties[a]		ASL	AIL	Hem	Cel	Ara	Gal	Man	Xyl	Glu	CWE	HWE
C0: Sound wood												
Sapwood	Mean	0.3	29.8	19.2	38.1	1.3	1.4	7.4	5.5	41.6	2.4	4.1
	SD[b]	0.0	0.9	1.1	1.3	0.1	0.2	0.3	0.3	1.4	0.8	1.1
Heartwood	Mean	0.5^{A}	30.1^{A}	15.5^{A}	38.8^{A}	1.0^{A}	2.4^{A}	7.2^{A}	4.4^{A}	41.9^{A}	4.3^{A}	9.8^{A}
	SD	0.05	0.77	1.1	1.0	0.1	0.7	0.9	0.5	1.2	0.6	0.8
C1: Initial stage of decay												
Heartwood	Mean	0.5^{A}	30.1^{A}	13.0^{B}	38.3^{A}	0.7^{B}	1.7^{B}	6.5^{A}	4.1^{A}	40.4^{A}	4.2^{A}	9.7^{A}
	SD	0.1	0.4	0.3	0.7	0.1	0.2	0.3	0.2	0.5	0.2	0.5
	R[c]	−2.1	−0.2	16.4	1.2	31.1	27.9	9.9	7.5	3.7	3.7	1.3
C2: Advanced stage of decay												
Heartwood	Mean	0.6^{A}	32.7^{A}	12.1^{B}	30.5^{B}	0.6^{C}	1.5^{C}	6.0^{A}	4.0^{A}	32.1^{B}	4.2^{A}	9.6^{A}
	SD	0.1	2	0.1	1.6	0.2	0.1	0.8	0.5	0.6	0.5	0.4
	R	−16.6	−9.3	22.1	21.4	42.7	35.8	16.7	8.9	23.5	3.9	2.6

Means with different letters are significantly different at $p < 0.05$.

[a] Properties: ASL = Acid soluble lignin; AIL = Acid insoluble lignin; Hem = Hemicelluloses; Cel = Cellulose; Ara = Arabinan; Gal = Galactan; Man = Mannan; Xyl = Xylan; Glu = Glucan; CWE = cold water extractives and HWE = hot water extractives.

[b] SD = Standard deviation.

[c] The reduction of ASL, AIL, Hem, Cel, Ara, Gal, Man, Xyl, Glu, CWE and HWE of decayed wood (C1 and C2) was calculated compared to mean ASL, AIL, Hem, Cel, Ara, Gal, Man, Xyl, Glu, CWE and HWE of sound sample (C0).

Table 4
Variation of mechanical properties and weight with decay class (C0, C1 and C2) in *Thuja occidentalis* L.

Tests	Three point bending test			Parallel compression		Perpendicular compression		Hardness (N)		
Properties[a]	MOE (MPa)	MOR (MPa)	Weight (g)	MS (MPa)	Weight (g)	LS (MPa)	Weight (g)	Surface	End	Weight (g)
C0: Sound wood										
Mean	5351^{A}	57.5^{A}	21.2^{A}	44.3^{A}	21.8^{A}	4.25^{A}	21.6^{A}	2035^{A}	1949^{A}	103.4^{A}
SD[b]	660	7.1	0.9	3.6	1.1	0.6	0.8	250	279	15.3
C1: Initial stage of decay										
Mean	4424^{B}	45.2^{B}	19.9^{A}	38.8^{B}	19.9^{A}	3.2^{B}	20^{A}	1630^{B}	1568^{B}	92.6^{A}
SD	126	4.2	3.2	3.0	0.7	0.2	0.3	84	68	12.3
R[c]	17.4	21.5	6.3	12.4	8.5	23.7	7.42	19.9	19.6	10.4
C2: Advanced stage of decay										
Mean	3726^{C}	35^{C}	18.2^{B}	34.3^{C}	18.4^{B}	2.7^{C}	18.7^{B}	1381^{C}	1297^{C}	85.2^{B}
SD	191	5	0.7	3.9	0.8	0.2	0.6	111	154	11.1
R	30.4	39.8	14.4	22.5	15.5	36.7	13.4	32.1	33.5	17.7

[a] Properties: MOE = Modulus of elasticity in bending; MOR = Modulus of rupture in bending; MS = Maximum compressive strength parallel to grain compression; LS = Stress at limit of elasticity in perpendicular compression; surface hardness and end hardness.
[b] SD = Standard deviation.
[c] The reduction of MOE, MOR, MS, LS, hardness and weights of decayed wood (C1 and C2) was calculated compared to mean MOE, MOR, MS, LS, hardness and weights of sound sample (C0). Means with different letters are significantly different at $p < 0.05$.

3.5. Impact of chemical changes on mechanical properties

Highly significant correlations were found between most mechanical properties and cellulose, hemicellulose, and carbohydrate content (Table 6). In particular, the coefficients of correlation between cellulose content and all mechanical properties were very high. The highest coefficients of correlation were found for MS ($r = 0.93$), followed by hardness ($r = 0.90$) and MOE ($r = 0.85$), whereas the least significant coefficient of correlation was found between cellulose content and MOR ($r = 0.49$). Strong correlations were also found between hemicellulose content and certain mechanical properties (Table 6), albeit generally lower than the correlations for cellulose content, except for the MOR ($r = 0.75$). In the relationships between carbohydrate content and mechanical properties, MOR was highly correlated with arabinan ($r = 0.60$) and galactan ($r = 0.65$), but weakly correlated with mannan, xylans, and glucan (Table 6). Table 6 also reveals a strong relationship between weight loss and mannan and xylan content, with a weak relationship between weight loss and arabinan and galactan content.

4. Discussion

4.1. Decayed wood structure

All changes in cell wall structure were closely related to fungal activity (Fig. 1). In the early stages of decay, the degradation was more extensive in earlywood than in latewood due to the narrow cell lumina and the thick cell walls characteristic of latewood (Fig. 1A). This result is in good agreement with previous reports on decay in other wood species (Schmitt et al., 2005; Schwarze, 2007). This early evidence of cell wall degradation in earlywood was attributed to a rapid decrease in the degree of polymerization of celluloses (Douglas et al., 1991; Schwarze, 2007). The lower degradation of latewood fibers appears to be related to higher cell wall lignification in the thick walls, which hampers the transfer of the cellulolytic enzyme produced by the fungal hyphae into the cell wall (Schwarze, 2007). Blanchette (2000) attributed this lower degradation to the narrow cell lumina, the thick cell walls, and the limited number of bordered pits in the latewood cell walls compared to earlywood, delaying the proliferation of decay.

Brown-rot decay appears to be unable to degrade the most lignin-rich part of the cell walls and the middle lamellae (Irbe et al., 2006, 2011). For this reason, the decay incidence varies with the cell types within wood (earlywood or latewood), and even within the wall layers of individual cells. In initial decay, the degradation is limited to cell lumina of the earlywood tracheids. This is considered an essential step to prevent decay activity (Schwarze, 2007). However, in advanced decay, the middle lamella becomes slightly altered, although cell walls are extensively degraded. During the maturation of woody cells, all the layers of the wall and the middle lamella are, to a greater or slighter extent, impregnated with lignin. Nevertheless, lignification is more pronounced in the compound middle lamella, where it can exceed 80% of the total compound content (Schwarze, 2007). This can explain why middle lamella is more resistant to decay (Kirk and Highley, 1973; Schmitt et al., 2005; Irbe et al., 2011). As decay progresses, the wood cell walls can crumble into fragments. This is the result of an extensive removal of cellulose and hemicelluloses of wood fibers, leaving an empty lignin skeleton. Without cellulose, wood fibers lack structural integrity, and the wood degradation subsequently spreads, forming holes and cracks (Schwarze, 2007; Moskal-del Hoyo et al., 2010).

Table 5
Ratio strength[a]/weight loss and correlations.[b]

Properties	Ratio strength/weight loss		Correlation
	C1	C2	
MOE	2.78:1	2.11:1	0.71***[c]
MOR	3.45:1	2.76:1	0.54***
MS	1.45:1	1.45:1	0.71***
LS	3.19:1	2.73:1	0.80***
Surface hardness	1.91:1	1.82:1	0.65***
End hardness	1.88:1	1.89:1	0.72***

[a] Strength properties: MOR = Modulus of rupture in bending; MOE = Modulus of elasticity in bending; MS = Maximum compressive strength parallel to grain compression; LS = Stress at limit of elasticity in perpendicular compression, surface hardness and end hardness.
[b] Correlation between weight loss and mechanical properties.
[c] Significance level: *** = $p < 0.001$. C1 = Initial stage of decay and C2 = Advanced stage of decay.

4.2. Changes in physical, chemical, and mechanical properties

The non-significant effect of site on RD, EWD, and LWD (Table 1) is surprising. It could be explained by the fact that the error term accounted for a high percentage of the total variation. This suggests that other factors not accounted for in this analysis may have

Table 6
Correlation between chemical composition and mechanical properties.

Properties[a]		Cell	Hem	Arab	Gal	Xyl	Man	Glu
Perpendicular compression	LS	0.83***[b]	0.66*	0.63**	0.65**	0.46*	0.72***	0.84***
	Weight	0.91***	0.41*	0.36^{ns}	0.33^{ns}	0.49*	0.58**	0.88***
Parallel compression	MS	0.93***	0.36^{ns}	0.63**	0.45^{ns}	0.45*	0.73***	0.90***
	Weight	0.87***	0.41*	0.36^{ns}	0.39*	0.42*	0.70***	0.84***
Bending three tests	MOE	0.85***	0.25^{ns}	0.70**	0.70**	0.43*	0.59**	0.86***
	MOR	0.49*	0.75***	0.6**	0.65**	0.28^{ns}	0.55*	0.59*
	Weight	0.76***	0.48*	0.33^{ns}	0.27^{ns}	0.44*	0.68***	0.79***
Hardness	Surface	0.90***	0.06^{ns}	0.71***	0.67**	0.39^{ns}	0.63**	0.94***
	End	0.89***	0.07^{ns}	0.64**	0.38^{ns}	0.49*	0.69**	0.88***
	Weight	0.84***	0.82***	0.75***	0.52**	0.49*	0.65**	0.89***

[a] Properties: MOE = Modulus of elasticity in bending; MOR = Modulus of rupture in bending; MS = Maximum compressive strength parallel to grain compression; LS = stress at limit of elasticity in perpendicular compression; surface hardness; end hardness; Cell = cellulose; Hem = hemicelluloses; Arab = Arabinan; Gal = Galactan; Xyl = xylan; Man = Mannan; Glu = glucan.
[b] Significance level: * = $p < 0.05$; ** = $p < 0.01$; *** = $p < 0.001$ and ns = non-significant.

influenced the variation in these properties. One possible factor is the variation in ring density components due to environmental conditions such as precipitation and temperature. In addition, the variations due to other factors, namely cambial age, decay, and tree-to-tree, were too large, which might have masked the site effect.

The significant effect of cambial age on RD and EWD was due to the juvenile variation for these traits. The analyzed rings had a cambial age ranging from 2 to 20, and the wood, which was mainly juvenile, varied widely in terms of cell dimensions and cell wall formation (Panshin and De Zeeuw, 1980).

The effect of tree on RD and EWD and LWD was also highly significant (Table 1). This was due to several factors, including microenvironmental soil conditions and other sources of phenotypic variation. Moreover, the significant effect of the Tree x Decay Class interaction (Table 1) suggests that the effect of decay varies among trees within the same site, which could be explained by the differences in intrinsic tree characteristics, including age, initial wood density, and chemical composition.

According to Table 2 and Fig. 2, the wood density components (RD, EWD, and LWD) decreased with increasing decay. However, changes in density due to decay were more prominent in earlywood than latewood tracheids. This early evidence of earlywood degradation agrees with the SEM results. This result could be explained by the fact that latewood has higher density (Fig. 2C), thicker cell walls, and narrower cell lumens than earlywood tracheids (Fig. 1A). The resistance of latewood is attributable to the higher lignification of cell walls, which helps reduce the wood degradation by decay (Schwarze, 2007; Irbe et al., 2011).

The interaction effect between cambial age and decay class was highly significant, and it contributed the most to the variation in RD and EWD (Table 1). This significant effect can be explained by the decrease in decay incidence from the pith outwards (Fig. 2 and Table 2). At all decay stages, the wood density loss due to decay was greater near the pith and decreased outwards (Table 2). The pattern of radial variation in wood density further shows that the degradation in both early and advanced decay stages occurred in the heartwood. The advanced decay stage was characterized by severe degradation near the pith, although the sapwood was free of apparent degradation. This can be explained by the unsuitability of functional sapwood for fungal establishment due to its high moisture content, low oxygen content (O_2), and lack of easily assimilable nutrients other than within living cells (Boddy and Rayner, 1983). In functional sapwood, decay development might be restricted by active defense mechanisms. However, decay can occur in sapwood when these limitations are removed by certain mechanisms such as drying or wounds, which prevent normal sapwood functioning (Boddy and Rayner, 1983). In service, the sapwood of most tree species has low extractive content, and is generally considered more susceptible to decay (Schwarze, 2007; Irbe et al., 2011).

According to the chemical results (Table 3), the extractive content of EWC (14.1%) was twice as high as that of southern pine and Engelmann spruce (Kirk and Highley, 1973), and higher than that of larch, at below 13% (Gierlinger et al., 2004). The xylans content of EWC (4.4%) was much lower than that of *Cedrus libani* (11%) (Blanchette, 2000). Lignin content (31.5%) was higher than that of larch species (25.9–29%) (Gierlinger et al., 2004). These species are known for their natural resistance to fungal decay (Kirk and Highley, 1973; Blanchette, 2000; Gierlinger et al., 2004).

The presence of decay was associated with a slight decrease in extractive content (Table 3). This suggests that decay fungi had difficulty attacking the extractives. However, decay fungi can degrade these compounds under certain combinations of environmental conditions, such as the presence of oxygen and moisture (Boddy and Rayner, 1983). Schultz and Nicholas (2000) reported that extractives may protect wood against fungal colonization and subsequent degradation by dual mechanisms: the extractives have some fungicidal activity and are also free radical antioxidants, which rapidly reduce hydroxyl radicals and could protect the cellulose fibers (Willför et al., 2003). The dual defense hypothesis is based on the fact that fungi could use some types of free radical species to initially disturb cell walls by increasing the pore size, which would then facilitate the diffusion of fungal enzymes into the cell walls. However, the phenolic extractives in heartwood are excellent antioxidants, and therefore probably contribute to the tree's chemical defence mechanisms (Willför et al., 2003). The initial step of decay is presumed to involve some types of free radicals (Arantes et al., 2012), which perturb the cell wall, and it is this early step in the decay process which may be inhibited by the antioxidant properties of the heartwood extractives (Schultz and Nicholas, 2000). The structure of wound-associated wood has been also studied in beech (Vek et al., 2013a,b) and results revealed that higher amounts of total phenols were characteristic of the reaction zone, and especially of wound-wood, while the lowest contents were measured in red heart samples.

Brown-rot decay destroyed the wood by selectively degrading the hemicelluloses and cellulose without removing the lignin (Table 3). These results are in good agreement with previous reports (Kirk and Highley, 1973; Douglas et al., 1991; Green III and Highley, 1997; Arantes et al., 2012). Decay removed the hemicelluloses more rapidly than cellulose during incipient decay (Table 3). These observations also agree with previous findings

(Kirk and Highley, 1973; Curling et al., 2002; Irbe et al., 2006). More cellulose was removed by brown-rot decay at the advanced decay stage (Table 3), suggesting a preferential degradation of cellulose. Fackler and Schwanninger (2010) reported a reduction in amorphous wood polysaccharides in preference to crystalline cellulose due to brown-rot decay.

In good agreement with previous reports (Jordan et al., 1996; Shimada et al., 1997), the increase in lignin content is attributable to the failure of fungi to attack lignin compared to polysaccharides. Thus, the increase of lignin content is mainly due to the decrease of polysaccharides' content. This increase could also be attributed to the formation of additional materials such as fungus products. Brown-rot fungi are known to cause rapid and extensive depolymerization of hemicelluloses and cellulose and to produce end products such as acid hydrolysis and oxalic acid. According to Oliveira et al. (2010), the decay caused by the rot fungi led to an increase in the proportion of cell-wall uronic acids, mainly due to the decrease in the relative percentage of xylans and mannans.

Lignin, a complex heterogeneous structural polymer, is present throughout the cell wall. Spatially, lignin is closely interspersed with hemicelluloses, forming a matrix that surrounds the cellulose microfibrils and provides a physical and chemical barrier to decay degradation (Ohkoshi et al., 1999). Thus, the presence of brown-rot decay provokes degradation of the hemicelluloses and cellulose of the cell wall (Fig. 1E), leaving the lignin undigested (Green III and Highley, 1997; Irbe et al., 2006, 2011; Yelle et al., 2008; Arantes et al., 2012).

The variation in the removal of carbohydrate components observed in this study, where arabinan and galactan were removed more rapidly than mannan, xylans, and glucan (Table 3), is in good agreement with that reported for southern pine (Curling et al., 2002), suggesting that cellulose and possibly some hemicelluloses (xylans) tolerate substantial depolymerization (Silva et al., 2007). Consequently, they degrade and are removed progressively (Green III and Highley, 1997).

Silva et al. (2007) attributed the changes in cell-wall polysaccharide composition of brown-rot decayed heartwood to the decrease in polymers other than xylans. The preferential depletion of mannan by brown-rot decay compared to xylans has been noted previously (Kirk and Highley, 1973; Irbe et al., 2006). However, the removal of xylans is still poorly understood, even though brown-rot fungi preferentially decomposed unsubstituted xylose units but partially decomposed the mono-substituted xylose units in acetylated wood (Ohkoshi et al., 1999). Mannan, a major hemicellulose component, was also removed faster than glucan (Table 3), suggesting that the degradation and removal of the cellulose may depend on prior removal of mannan. Hemicelluloses develop an encrusting envelope around the cellulose microfibrils. Consequently, the degradation and removal of cellulose may well require prior removal of hemicelluloses (Kirk and Highley, 1973; Clausen and Kartal, 2003). In summary, mannans are removed faster than xylans, and both types of hemicelluloses are removed faster than cellulose (Green III and Highley, 1997; Curling et al., 2002).

The greater galactan and arabinan loss compared to mannan and xylans suggests selective degradation of the galacto-glucomannan and arabino-glucoronoxylan components, which has been previously anticipated, although the degradation process remains unclear (Winandy and Morrell, 1993).

Table 4 also shows a significant negative impact of brown-rot decay on all tested mechanical properties. In good agreement with Curling et al.'s (2002) results, MOR decreased more rapidly than MOE. The presence of decay was accompanied by substantial decreases in mechanical properties as a result of only modest losses in weight (Tables 4 and 5). This result supports the findings of Wilcox (1978), who reported that only a modest weight loss (5%) significantly reduced mechanical properties. This result has important practical implications indicating that wood showing signs of presence of even early stages of decay will make the wood weak and unsuitable for structural applications.

The relative ratios for loss in mechanical properties to weight loss found in this study (Table 5) were lower than those for southern pine sapwood exposed to brown-rot fungi (*Gloeophyllum trabeum*), where the loss in mechanical properties of sapwood relative to weight loss (5%) was 4.5:1 for MOR and 3.5:1 for MOE (Curling et al., 2002). For the same weight loss, this ratio was 6:1 for MOR after 4-week incubation of southern yellow pine blocks exposed to *Postia placenta* (Clausen and Kartal, 2003). Thus, loss of mechanical properties in EWC wood is not as rapid as that for southern pine wood.

Strong relationships were also found between most mechanical properties and weight loss (Table 5). However, it also emerged that mechanical property losses in EWC wood were not as rapid as in Douglas-fir (Smith and Graham, 1983). In southern pine sapwood exposed to brown-rot fungi (*G. trabeum*), the weight loss varied from 5 to 20% as decay progressed. This variation was associated with significant changes in mechanical properties, with losses from 40 to 80% for MOR and 25–70% for MOE (Curling et al., 2002), compared to 39.8% for MOR and 30.4% for MOE at 15% weight loss in EWC (Table 4).

4.3. Relationships between chemical changes and mechanical properties due to decay

During the decay process, mechanical properties were significantly correlated to cellulose, hemicellulose, and carbohydrate content (Table 6). In good agreement with previous reports (Winandy and Morrell, 1993; Curling et al., 2002), MOR was weakly correlated to cellulose content (Table 6), but strongly correlated to hemicellulose content (Table 6). This supports Kartal et al.'s (2008) findings of a strong correlation between hemicellulose content and MOR loss during thermal degradation of sugi (*Cryptomeria japonica* D. Don) sapwood.

In contrast, a strong relationship was found between MOE and cellulose, indicating that wood stiffness is more dependent on cellulose content, whereas wood strength (MOR) is more dependent on hemicelluloses (Table 6). In addition, the strong relationships between MOR and arabinan and galactan content compared to mannan and xylans content (Table 6) indicate that MOR is more dependent on arabinan and galactan content. Thus, MOR increased as arabinan and galactan content decreased. This sheds light on the previously discussed results (Sections 3.3, 3.4, and 4.2), and explains why MOR loss was greater than MOE loss at the early stage of decay (Table 4). Initial decay was associated with substantial losses in arabinan and galactan content (Table 3). Arabinan was the most degraded (42.7%) carbohydrate component at advanced decay (Table 3). However, at approximately 40% MOR loss (Table 4), only 16.7% of the mannan and 8.9% of the xylans was degraded, which can explain the weaker relationship found between MOR and the mannan and xylan components (Table 6). Consequently, the strong relationship between the mechanical and chemical properties suggests that the loss of mechanical properties (Table 4) due to decay resulted from the loss of specific compounds in the polysaccharides (Table 3).

The results also show that weight loss was strongly correlated to mannan and xylans content, but weakly correlated to arabinan and galactan content (Table 6). Mannan and xylans accounted for approximately 18% of the wood content compared to 8% for galactan and arabinan (Highley, 1987; Curling et al., 2002). This explains the relationship between mannan and xylans weight loss.

Consequently, the presence of decay induced substantial losses in strength properties despite the relatively low weight loss.

5. Conclusions

Changes in anatomical, physical, chemical, and mechanical properties due to brown-rot decay in *T. occidentalis* L. wood were investigated. The following conclusions can be drawn:

1. Decay incidence varied with cell types and within wood. In the early stages of decay, degradation was limited to the cell lumina of the earlywood tracheids, whereas in advanced stages of decay, wood degradation was observed in both earlywood and latewood tracheids.
2. Changes in wood density due to decay were more prominent in earlywood than latewood tracheids. Wood degradation was severe near the pith and the decay was limited to the heartwood. The living sapwood was free from decay due to the unsuitability of functional sapwood for mycelial establishment.
3. Brown-rot decay destroyed the wood by selectively degrading the hemicelluloses and cellulose without removing the lignin. Arabinan and galactan were destroyed faster than mannan and xylans, and hemicelluloses faster than cellulose.
4. Brown-rot decay led to a substantial reduction in the wood mechanical properties. This decrease was mainly explained by decay-induced chemical changes.

Acknowledgments

The authors thank the Canada Research Chair Program, the Ministère des ressources naturelles et de la faune, Quebec (MRNF), and the NSERC-UQAT-UQAM Industrial chair on forest sustainable management for funding this project.

References

Amusant, N., Beauchene, J., Fournier, M., Janin, G., Thevenon, M.F., 2004. Decay resistance in *Dicorynia guianensis* Amsh: analysis of inter-tree and intra-tree variability and relations with wood colour. Ann. For. Sci. 61, 373–380.

Amusant, N., Moretti, C., Richard, B., Prost, E., Nuzillard, J.M., Thévenon, M.F., 2007. Chemical compounds from *Eperua falcata* and *Eperua grandiflora* heartwood and their biological activities against wood destroying fungus (*Coriolus versicolor*). Holz Roh Werkst. 65, 23–28.

Arantes, V., Jellison, J., Goodell, B., 2012. Peculiarities of brown-rot fungi and biochemical Fenton reaction with regard to their potential as a model for bioprocessing biomass. Appl. Microbiol. Biotechnol. 94, 323–338.

Behr, E.A., 1976. Special physical and chemical properties of northern white cedar. In: Proceedings of the National Northern White Cedar Conference, vol. 3–76. Michigan State University Publication, East Lansing, p. 11–15.

Blanchette, R.A., 2000. A review of microbial deterioration found in archaeological wood from different environments. Int. Biodeterior. Biodegrad. 46, 189–204.

Boddy, L., Rayner, A.D.M., 1983. Origins of decay in living deciduous trees: the role of moisture content and a re-appraisal of the expanded concept of tree decay. New Phytol. 94, 623–641.

Bouslimi, B., Koubaa, A., Bergeron, Y., 2013. Variation of brown rot decay in eastern white cedar (*Thuja occidentalis* L.). BioResources 8, 4735–4755.

Browning, B.L., 1967. Methods of Wood Chemistry, vol. II. Interscience, New York.

Clausen, C.A., Kartal, S.N., 2003. Accelerated detection of brown-rot decay: comparison of soil block test, chemical analysis, mechanical properties, and immunodetection. For. Prod. J. 53, 90–94.

Curling, S.F., Clausen, C.A., Winandy, J.E., 2002. Relationships between mechanical properties, weight loss, and chemical composition of wood during incipient brown-rot decay. For. Prod. J. 52, 34–39.

Curnel, Y., Jacques, D., Gierlinger, N., Pĝques, L.E., 2008. Variation in the decay resistance of larch to fungi. Ann. For. Sci. 65.

Douglas, S., Flournoy, T.K.K., Highley, T.L., 1991. Wood decay by brown-rot fungi: changes in pore structure and cell wall volume. Holzforschung 45, 383–388.

Fackler, K., Schwanninger, M., 2010. Polysaccharide degradation and lignin modification during brown rot of spruce wood: a polarised Fourier transform near infrared study. J. Near Infrared Spectrosc. 18, 403–416.

Fowells, H.A. (Ed.), 1965. Silvics of Forest Trees of the United States. Department of Agriculture, United States, p. 271. Agriculture Handbook.

Gierlinger, N., Jacques, D., Schwanninger, M., Wimmer, R., Pâques, L., 2004. Heartwood extractives and lignin content of different larch species (*Larix* sp) and relationships to brown-rot decay-resistance. Trees – Struct. Funct. 18, 230–236.

Grabner, M., Wimmer, R., Gierlinger, N., Evans, R., Downes, G., 2005. Heartwood extractives in larch and effects on X-ray densitometry. Canad. J. For. Res. 35, 2781–2786.

Green III, F., Highley, T.L., 1997. Mechanism of brown-rot decay: paradigm or paradox. Int. Biodeterior. Biodegrad. 39, 113–124.

Guller, B., Isik, K., Cetinay, S., 2012. Variations in the radial growth and wood density components in relation to cambial age in 30-year-old *Pinus brutia* Ten. at two test sites. Trees – Struct. Funct., 1–12.

Haataja, B.A., Laks, P.E., 1995. Properties of flakeboard made from northern white cedar. For. Prod. J. 45, 68–70.

Hastrup, A.C.S., Howell, C., Larsen, F.H., Sathitsuksanoh, N., Goodell, B., Jellison, J., 2012. Differences in crystalline cellulose modification due to degradation by brown and white rot fungi. Fungal Biol. 116, 1052–1063.

Highley, T.L., 1987. Changes in chemical components of hardwood and softwood by brown-rot fungi. Mater. Organism. 22, 39–45.

Hofmeyer, P.V., Seymour, R.S., Kenefic, L.S., 2009. Influence of soil site class on growth and decay of northern white-cedar and two associates in Maine. North. J. Appl. For. 26, 68–75.

Howell, C., Hastrup, A.C.S., Jara, R., Larsen, F.H., Goodell, B., Jellison, J., 2011. Effects of hot water extraction and fungal decay on wood crystalline cellulose structure. Cellulose 18, 1179–1190.

Irbe, I., Andersone, I., Andersons, B., Noldt, G., Dizhbite, T., Kurnosova, N., Nuopponen, M., Stewart, D., 2011. Characterisation of the initial degradation stage of Scots pine (*Pinus sylvestris* L.) sapwood after attack by brown-rot fungus *Coniophora puteana*. Biodegradation 22, 719–728.

Irbe, I., Andersons, B., Chirkova, J., Kallavus, U., Andersone, I., Faix, O., 2006. On the changes of pinewood (*Pinus sylvestris* L.) Chemical composition and ultrastructure during the attack by brown-rot fungi *Postia placenta* and *Coniophora puteana*. Int. Biodeterior. Biodegrad. 57, 99–106.

Johnston, W.F., Booker, R.G., 1983. Northern white cedar. In: Burns, R.M. (Ed.), Silvicultural Systems for the Major Forest Types of the United States. Washington, DC, USDA Forest Service, Agriculture Handbook, 445, p. 105–108.

Jordan, C.R., Dashek, W.V., Highley, T.L., 1996. Detection and quantification of oxalic acid from the brown-rot decay fungus, *Postia placenta*. Holzforschung 50, 312–318.

Kartal, S.N., Hwang, W.-J., Imamura, Y., 2008. Combined effect of boron compounds and heat treatments on wood properties: chemical and strength properties of wood. J. Mater. Process. Technol. 198, 234–240.

Kirk, T.K., Highley, T.L., 1973. Quantitative changes in structural components of conifer woods during decay by white- and brown-rot fungi. Phytopathology 63, 1338–1342.

Kleist, G., Schmitt, U., 2001. Characterisation of a soft rot-like decay pattern caused by *Coniophora puteana* (Schum.) Karst. in Sapelli wood (*Entandrophragma cylindricum* Sprague). Holzforschung 55, 573–578.

Kleist, G., Seehann, G., 1997. Colonization patterns and topochemical aspects of sap streak caused by *Stereum sanguinolentum* in Norway spruce. Eur. J. For. Pathol. 27, 351–361.

Koubaa, A., Zhang, S.Y., Makni, S., 2002. Defining the transition from earlywood to latewood in black spruce based on intra-ring wood density profiles from X-ray densitometry. Ann. For. Sci. 59, 511–518.

Koubaa, A., Zhang, S.Y., White Cedar, Thuja occidentalis L. In: Zhang S.Y., and Koubaa, A. (Eds.) Softwoods of Eastern Canada. Their Sylvics, characteristics, Manufacturing and End-Uses. Special Publication, SP-526E, Chapter 11, 2008, 18 p., FPInnovations, (Eds), Québec, Canada.

Koubaa, A., Zhang, S.Y., Isabel, N., Beaulieu, J., Bousquet, J., 2000. Phenotypic correlations between juvenile-mature wood density and growth in black spruce. Wood Fiber Sci. 32, 61–71.

Littell, R.C., Milliken, G.A., Stroup, W.W., Wolfinger, R.D., Schabenberber, O. (Eds.), 2006. SAS for Mixed Models Second Edition. SAS Institute, Inc, Cary, NC, p. 814.

Martínez, Á.T., Speranza, M., Ruiz-Dueñas, F.J., Ferreira, P., Camarero, S., Guillén, F., Martínez, M.J., Gutiérrez, A., Río, J.C.d., 2005. Biodegradation of lignocellulosics: microbial, chemical, and enzymatic aspects of the fungal attack of lignin. Int. Microbiol. 8, 195–204.

Moskal-del Hoyo, M., Wachowiak, M., Blanchette, R.A., 2010. Preservation of fungi in archaeological charcoal. J. Archaeol. Sci. 37, 2106–2116.

Ohkoshi, M., Kato, A., Suzuki, K., Hayashi, N., Ishihara, M., 1999. Characterization of acetylated wood decayed by brown-rot and white-rot fungi. J. Wood Sci. 45, 69–75.

Oliveira, L.S., Santana, A.L.B.D., Maranhão, C.A., de Miranda, R.D.C.M., Galvão de Lima, V.L.A., da Silva, S.I., Nascimento, M.S., Bieber, L., 2010. Natural resistance of five woods to *Phanerochaete chrysosporium* degradation. Int. Biodeterior. Biodegrad. 64, 711–715.

Panshin, A.J., De Zeeuw, C., 1980. Textbook of Wood Technology. McGraw-Hill Book Co., New York, p. 772.

Rowell, R.M., Roger, P., Han, J.S., Rowell, J.S., Tshabalala, M.A. (Eds.), 2005. Cell Wall Chemistry. CRC Press, Boca Raton, Fla.

SAS, 2008. SAS Institute Inc, Cary, NC.

Schilling, J., Tewalt, J., Duncan, S., 2009. Synergy between pretreatment lignocellulose modifications and saccharification efficiency in two brown rot fungal systems. Appl. Microbiol. Biotechnol. 84, 465–475.

Schmitt, U., Singh, A.P., Thieme, H., Friedrich, P., Hoffmann, P., 2005. Electron microscopic characterization of cell wall degradation of the 400,000-year-old wooden Schöningen spears. Holz Roh Werkst. 63, 118–122.
Schultz, T.P., Nicholas, D.D., 2000. Naturally durable heartwood: evidence for a proposed dual defensive function of the extractives. Phytochemistry 54, 47–52.
Schwarze, F.W.M.R., 2007. Wood decay under the microscope. Fungal Biol. Rev. 21, 133–170.
Shimada, M., Akamtsu, Y., Tokimatsu, T., Mii, K., Hattori, T., 1997. Possible biochemical roles of oxalic acid as a low molecular weight compound involved in brown-rot and white-rot wood decays. J. Biotechnol. 53, 103–113.
Silva, C.A.d., Beatriz Bacellar Monteiro, M., Brazolin, S., Antonio Carballeira Lopez, G., Richter, A., Braga, M.R., 2007. Biodeterioration of brazilwood *Caesalpinia echinata* Lam. (Leguminosae—Caesalpinioideae) by rot fungi and termites. Int. Biodeterior. Biodegrad. 60, 285–292.
Silva Pereira, C.M., Soares, G.A., Oliveira, A.C., Emília Rosa, M., Pereira, H., Moreno, N., Vitória San Romão, M., 2006. Effect of fungal colonization on mechanical performance of cork. Int. Biodeterior. Biodegrad. 57, 244–250.
Smith, S.M., Graham, R.D., 1983. Relationship between early decay and radial compression strength of Douglas-fir. For. Prod. J. 33, 49–52.
Syafii, W., Yoshimoto, T., 1991. Effect of lignin structure on decay resistance of some tropical woods. Indones. J. Trop. Agric. 3, 32–37.
T207, T, 1989. TAPPI T207 om-88. Water solubility and wood pulp. In: TAPPI Test Method, vol. I. TAPPI Press, Atlanta, USA.
T222, T, 1989. TAPPI T 222 om-88. Acid-insoluble lignin in wood and pulp. In: TAPPI Test Method, vol. I. TAPPI Press, Atlanta, USA.
T249, T, 1989. T249 cm-85. Carbohydrate composition of extractive-free wood and wood pulp by gas–liquid chromatography. In: TAPPI Test Method, vol. I. TAPPI Press, Atlanta, USA.
T264, T, 1989. TAPPI T264 om-88. Preparation of wood for chemical analysis. In: TAPPI Test Method, vol. I. TAPPI Press, Atlanta, USA.
Taylor, A.M., Gartner, B.L., Morrell, J.J., 2002. Heartwood formation and natural durability – a review. Wood Fiber Sci. 34, 587–611.
Taylor, A.M., Gartner, B.L., Morrell, J.J., Tsunoda, K., 2006. Effects of heartwood extractive fractions of *Thuja plicata* and *Chamaecyparis nootkatensis* on wood degradation by termites or fungi. J. Wood Sci. 52, 147–153.
Timell, T.E., 1957. Carbohydrate composition of ten North American species of wood. Tappi 40, 568–572.
Vek, V., Oven, P., Humar, M., 2013a. Phenolic extractives of wound-associated wood of beech and their fungicidal effect. Int. Biodeterior. Biodegrad. 77, 91–97.
Vek, V., Oven, P., Poljanšek, I., 2013b. Content of total phenols in red heart and wound-associated wood in beech (*Fagus sylvatica* L.) (Sadržaj ukupnih fenola u crvenom srcu i ranjenom dijelu drva bukve (*Fagus sylvatica* L.)). Drvna Industrija 64, 25–32.
Wan, H., Wang, X.M., Yang, D.Q., 2007. Utilizing eastern white cedar to improve the resistance of strand boards to mold and decay fungi. For. Prod. J. 57, 54–59.
Wilcox, W.W., 1978. Review of literature on the effects of early stages of decay on wood strength. Wood Fiber Sci. 9, 252–257.
Willför, S.M., Ahotupa, M.O., Hemming, J.E., Reunanen, M.H.T., Eklund, P.C., Sjöholm, R.E., Eckerman, C.S.E., Pohjamo, S.P., Holmbom, B.R., 2003. Antioxidant activity of knotwood extractives and phenolic compounds of selected tree species. J. Agric. Food Chem. 51, 7600–7606.
Willför, S., Sundberg, A., Hemming, J., Holmbom, B., 2005. Polysaccharides in some industrially important softwood species. Wood Sci. Technol. 39, 245–257.
Winandy, J.E., Morrell, J.J., 1993. Relationship between incipient decay, strength, and chemical composition of Douglas-fir heartwood. Wood Fiber Sci. 25, 278–288.
Yang, Z., Ren, H.Q., Jiang, Z.H., 2010. Effects of biological decay on mechanical properties of slash pine wood. J. Beijing Forestry Univ. 32, 146–149.
Yelle, D.J., Ralph, J., Lu, F., Hammel, K.E., 2008. Evidence for cleavage of lignin by a brown rot basidiomycete. Environ. Microbiol. 10, 1844–1849.